

Toward Understanding Liposome-Based siRNA Delivery Vectors: Atomic-Scale Insight into siRNA–Lipid Interactions

Alexandra Yu. Antipina[†] and Andrey A. Gurtovenko^{*,‡,§} 

[†]Department of Photonics and Optical Information Technology, ITMO University, 49 Kronverksky Pr., St. Petersburg 197101, Russia

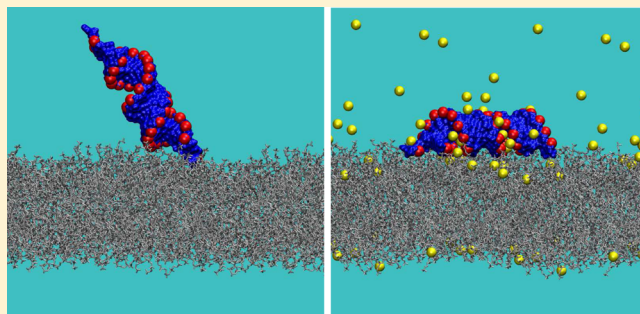
[‡]Institute of Macromolecular Compounds, Russian Academy of Sciences, Bolshoi Prospect V.O. 31, St. Petersburg 199004, Russia

[§]Faculty of Physics, St. Petersburg State University, Ulyanovskaya Street 3, Petrodvorets, St. Petersburg 198504, Russia

Supporting Information

ABSTRACT: Liposome carriers for delivering small interfering RNA (siRNA) into target cells are of tremendous importance because the siRNA-based therapy offers a completely new approach for treating a wide range of diseases, including cancer and viral infections. In this paper, we employ the state-of-the-art computer simulations to get an atomic-scale insight into the interactions of siRNA with zwitterionic (neutral) lipids. Our computational findings clearly demonstrate that siRNA does adsorb on the surface of a neutral lipid bilayer. The siRNA adsorption, being rather weak and unstable, is driven by attractive interactions of overhanging unpaired nucleotides with choline moieties of lipid molecules.

It is the presence of the unpaired terminal nucleotides that underlies a drastic difference between siRNA and DNA; the latter is not able to bind to the zwitterionic lipid bilayer. We also show that adding divalent Ca ions leads to the formation of stable siRNA–lipid system complexes; these complexes are stabilized by Ca-mediated aggregates of siRNA and lipid molecules rather than by the overhanging siRNA nucleotides. Furthermore, the molecular mechanism of interactions between siRNA and the lipid bilayer in the presence of divalent cations seems to involve exchange of Ca ions between the outer mouth of the major groove of siRNA and the lipid/water interface. Overall, our findings contribute significantly to a deeper understanding of the structure and function of liposome carriers used for siRNA delivery and can be used as a theoretical basis for further development of siRNA-based therapeutics.



INTRODUCTION

Since its discovery,¹ the RNA interference has attracted a great deal of attention from both the scientific community and pharmacological companies as it offers a completely new approach for treating a wide range of diseases, including cancer and viral infections. The small interfering RNA (siRNA) therapy largely relies on post-transcriptional silencing of target genes; some of the siRNA-based therapeutics are currently in the final stages of clinical trials.^{2,3} Similar to other types of nucleic acids, the use of siRNA as drug molecules suffers from several severe limitations such as poor cellular uptake as well as rapid degradation and clearance. A standard approach to overcome these limitations is to use delivery vectors that protect the nucleic acid and enhance its bioavailability. For instance, numerous nonviral delivery systems have been designed for DNA-based gene therapy, including liposomes, polyplexes, and inorganic nanoparticles.^{4,5} Most of these DNA delivery vectors can also be applied to siRNA delivery.^{6–8}

Lipid-based carriers are one of the most widely used delivery vehicles for siRNA delivery. In particular, cationic lipids are shown to be effective in increasing the siRNA cellular uptake⁹ at the cost of their rather high toxicity.¹⁰ As a much safer

alternative, zwitterionic (neutral) lipids could be used instead of cationic ones as they represent natural components of cell membranes. Such neutral lipids are often included in liposomal formulations as “helper lipids” to improve the liposome stability.¹¹ Remarkably, there are strong experimental evidences that siRNA delivery vectors based on zwitterionic liposomes are able to demonstrate high antitumor efficacy.¹² In some cases (e.g., for DOPC lipids) neutral liposomes are 10 times more effective in siRNA delivery as compared to their cationic counterparts (DOTAP lipids).¹³ Therefore, interactions of siRNA with zwitterionic lipids could be a key for developing safe and highly efficient siRNA therapeutics. Another important aspect in “lipid–nucleic acid” interactions is related to the role of salt ions. In particular, numerous experiments showed that attractive interactions between DNA and zwitterionic lipid molecules could be promoted in the presence of divalent cations such as calcium.^{14–18} Because RNAs are also polyanionic molecules, one could expect similar calcium-related

Received: April 12, 2018

Revised: June 15, 2018

Published: June 22, 2018

effects also for siRNA–lipid systems. Despite the tremendous importance of zwitterionic phospholipid molecules for the development of siRNA delivery systems of low toxicity, siRNA–lipid interactions are still poorly understood, especially at a molecular level.

A siRNA molecule represents a short double-stranded helix (20–25 base pairs) with two overhanging unpaired nucleotides on each end of the molecule. Its small size makes siRNA an excellent object for studying through atomistic molecular dynamics (MD) simulations. Such simulations are able to provide an unprecedented high-resolution insight into the system in question and have successfully been applied to explore supramolecular complexes of siRNA with linear and hyperbranched cationic polymers.^{19–21} As far as phospholipid molecules are concerned, there has been a very limited number of computational studies that dealt with siRNA–lipid systems. The study by Tarek et al.²² focused mostly on translocation of a siRNA molecule through a water pore in a zwitterionic lipid bilayer driven by an external electric field. Interestingly, the authors reported that a siRNA molecule remained attached to the bilayer surface after the electric field was switched off, which could be a sign of attractive interactions between siRNA and lipid head groups.²² Another MD simulation study explored the effect of siRNA adsorption on the phase behavior of a lipid bilayer but the siRNA–lipid interactions were not characterized.^{22,23} To the best of our knowledge, the above two studies are the only publications to date which considered siRNA–lipid systems at atomistic resolution.

The present paper is the first computational study that focuses specifically on molecular mechanisms behind the interactions of siRNA with zwitterionic phospholipid bilayers. To this end, we employ atomic-scale MD simulations to get a detailed insight into the role of different sites of a siRNA molecule (the duplex and the overhanging unpaired nucleotides) in the siRNA binding to the lipid bilayer surface. Furthermore, we demonstrate for the first time that the presence of divalent calcium ions strengthens considerably attractive interactions between siRNA and the lipid bilayer. Although the calcium-induced effects are in general similar to those reported for DNA, there are important differences dictated by the geometry of the RNA double-stranded helix region (the A-form). Overall, our results contribute significantly to a deeper understanding of nucleic acid–lipid interactions and can be useful for further development of siRNA-based therapeutics.

METHODS

We have performed atomic-scale MD simulations of a siRNA molecule placed in the aqueous solution next to the surface of a palmitoyl-oleoyl-phosphatidylcholine (POPC) lipid bilayer. A siRNA molecule was oriented parallel to the bilayer; the initial siRNA–bilayer distance was defined as a distance between the closest atoms of siRNA and lipids along the bilayer normal and varied from 0.5 to 2 nm. siRNA–bilayer systems with and without calcium cations were considered; for each system type, the simulations were repeated twice with different initial siRNA–bilayer distances to improve the statistical reliability of the results (see Table 1).

Each simulated system consisted of a single siRNA molecule and a POPC bilayer of 288 lipids. As for the siRNA, we considered a 20 base-pair double-stranded siRNA sequence with two overhanging unpaired nucleotides (*dsAGACAGCAUAAUUGCUGUCU-ssUU*)₂ (total charge of $-42e$); such a siRNA molecule was considered in earlier MD simulation studies.^{22,23} The initial configuration of the siRNA in the A-form was generated with the use of the make-na server (<http://structure.usc.edu/make-na/server.html>).

Table 1. Simulated siRNA–Lipid Bilayer Systems

system	initial distance [nm]	CaCl ₂ salt [mM]	simulation time [μs]
siRNA–POPC-1	1		0.8
siRNA–POPC-2	2		0.8
siRNA–POPC–Ca-1	1	100	1.5
siRNA–POPC–Ca-2	0.5	100	1.5

structure.usc.edu/make-na/server.html). Because in calcium-free systems, one can anticipate a complete detachment of a siRNA molecule from the bilayer surface, the size of a simulation box was enlarged along the bilayer normal in such a way that siRNA could not interact simultaneously with the bilayer and its periodic image. More specifically, the box size was approximately 9 nm \times 10.5 nm \times 14 nm. The lipid bilayer, being \sim 4 nm thick, was in the XY-plane, so that the size of the water phase (and correspondingly the distance between the bilayer and its periodic image) was around 10 nm along the bilayer normal (the Z-axis). Given that the end-to-end vector of a siRNA molecule was \sim 7.3 nm, siRNA always interacted with one bilayer only. Note that after detachment from the bilayer leaflet, a siRNA molecule was able in some occasions to approach the opposite leaflet.

In turn, similar to Ca-induced adsorption observed in DNA–lipid systems,^{24,25} such a siRNA detachment is unlikely in the presence of calcium cations, so that one can use smaller box sizes for the siRNA–POPC–Ca systems. Therefore, the box size along the Z-axis was reduced to \sim 12.4 nm. The prepared siRNA–bilayer systems were solvated with \sim 31 000 (Ca-free systems) and \sim 25 000 (systems with 100 mM of CaCl₂) water molecules. Forty-two Na⁺ ions were used as siRNA counterions; 45 Ca²⁺ and 90 Cl⁻ ions were added in the siRNA–POPC–Ca systems. The total number of atoms amounted to 134 000 and 115 000 for the siRNA–POPC and siRNA–POPC–Ca systems, respectively.

siRNA was described in the framework of the ff99bsc0 χ_{OL3} force field; it is based on the AMBERff99 force field²⁶ with α/γ^{27} and χ_{OL3}^{28} reparameterizations. In turn, the AMBER lipid14 force field was used for POPC lipids.²⁹ Water molecules were represented by the TIP3P model;³⁰ standard AMBER parameters were used for ions.^{24–26}

The systems were simulated in the NpT ensemble at $T = 303$ K and $P = 1$ bar. The velocity-rescaling thermostat was used to maintain the temperature constant.³¹ Pressure was controlled anisotropically through the Berendsen scheme.³² The Lennard-Jones interactions were cut off at 1 nm; the particle-mesh Ewald method was used to handle the electrostatic interactions.³³ The time step was 2 fs. The frames were written into the trajectory every 50 ps. Calcium-free systems were simulated for 0.8 μ s, whereas the siRNA–POPC–Ca systems required longer time to equilibrate, so that the corresponding simulations were extended up to 1.5 μ s (see Table 1). All of the simulations were performed with the use of the Gromacs 4.5.6 suite.³⁴

Both siRNA and lipid models used in the study were validated against experimental and computational data available. On the basis of a 200 ns long simulation of a free-standing POPC bilayer, the area per lipid was found to be 0.65 ± 0.01 nm², which is in good agreement with experiments.³⁵ In turn, for siRNA, we used the recent force-field ff99bsc0 χ_{OL3} ²⁷ with improved parameters for glycosidic torsion angle χ . This allowed us to avoid structural deformations of a siRNA molecule as well as formation of artificial “ladder-like” structures.³⁶ The structure of the siRNA duplex was found to be stable in all Ca-free simulations; the corresponding helix parameters such as the helical twist (\sim 30) and the widths of the major and minor grooves (1.55 and 1.58 nm, respectively) agreed well with experimental data.²⁷

RESULTS AND DISCUSSION

siRNA Adsorption on Zwitterionic Phospholipid Bilayers. To study adsorption of a siRNA molecule on a lipid bilayer, a nucleic acid was initially placed parallel to the bilayer surface. We performed two independent MD simulations for the systems with the initial siRNA–bilayer distance

equal to 1 and 2 nm (see Table 1). Because most findings observed for the two systems turned out to be very similar, below we present results for the siRNA–POPC-1 system.

To follow the process of adsorption, we calculated the distance between centers of mass (COMs) of a siRNA molecule and a lipid bilayer as well as the corresponding characteristics for terminal nucleotides of siRNA strands (see Figure 1).

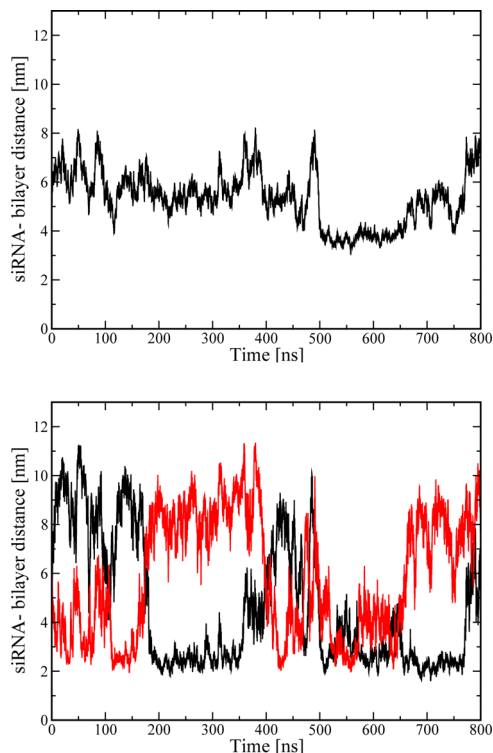


Figure 1. (Top) Time evolution of the distance between COMs of a siRNA molecule and a lipid bilayer along the bilayer normal. (Bottom) Time evolution of the COM distances between a lipid bilayer and terminal nucleotides of the first (U22-1, red line) and second (U22-2, black line) strands of siRNA.

Furthermore, a series of representative snapshots of the siRNA molecule interacting with the lipid bilayer surface are shown in Figure 2. First of all, one can see that siRNA does interact with the surface of a zwitterionic lipid bilayer, although its binding is relatively unstable: there are considerable fluctuations of the siRNA–bilayer distance with time. Figure 1 also highlights an important role of siRNA overhanging nucleotides in the interactions of siRNA with lipid molecules: most of the time at least one of the siRNA ends is anchored to the bilayer surface (see Figures 1 and 2). Such anchoring could last for more than 100 ns, followed by switching of the siRNA end anchoring to

the bilayer; this switching could be mediated by a complete temporary detachment of siRNA from the bilayer surface (see Figure 1 at $t = 170$ ns and Figure 2d). In contrast to the detachment, there are time intervals when both siRNA ends are bound to the bilayer surface and, correspondingly, the siRNA duplex as a whole is forced to adsorb on the lipid bilayer [see Figure 1 (500–650 ns) and Figure 2b].

Remarkably, the observed adsorption of siRNA on a zwitterionic lipid bilayer differs considerably from what was reported for DNA. Both experimental¹⁴ and computational²⁴ studies demonstrated that DNA does not adsorb onto the neutral lipid bilayer, unless divalent cations are present in the aqueous solution. Furthermore, our recent free-energy calculation showed that a zwitterionic phospholipid bilayer represents a repulsive barrier for DNA molecules.²⁵ Overall, one can conclude that the observed drastic difference between the ability of siRNA and DNA to adsorb on the bilayer surface is due to unpaired overhanging nucleotides at the ends of siRNA strands: the electronegative atoms of these nucleotides seem to interact favorably with polar head groups of zwitterionic lipids. Another aspect that can be of importance is related to the difference in native conformations of DNA (the B-form) and the duplex region of siRNA (the A-form). The B-form duplex is characterized by wider major grooves and narrower minor grooves as compared to the A-form counterpart. The width of the grooves could affect the interactions of ions with the duplex³⁷ and correspondingly the binding of the duplex to the lipid bilayer surface.

After we established that siRNA could adsorb on the surface of a zwitterionic lipid bilayer, we can now take advantage of atomistic models employed in simulations in order to gain a microscopic insight into the siRNA–lipid interactions. To this end, we considered various types of contacts between a siRNA molecule and POPC lipids. As siRNA is a polyanionic molecule with negative charges located on its phosphate groups (Prna), we start with the interactions of Prna and nitrogen atoms of oppositely charged choline moieties of zwitterionic POPC lipids (Npc). To calculate the number of the Prna–Npc contacts (as well as contacts of any other pairs of atoms), we follow closely the procedure outlined in our previous studies.^{24,38} First, we compute the radial distribution function (RDF) for Prna and Npc atoms (see Figure 3); the position of the first minimum of the RDF (0.6 nm) gives us the radius of the first coordination sphere of Prna with respect to Npc. The number of Prna–Npc contacts is then calculated by counting the number of Npc atoms within the first coordination sphere of Prna atoms.^{24,38}

As emphasized above, the overhanging unpaired nucleotides seem to play an important role in the siRNA adsorption. Therefore, it is instructive to distinguish the contacts of lipid choline groups with phosphate groups of the siRNA duplex and

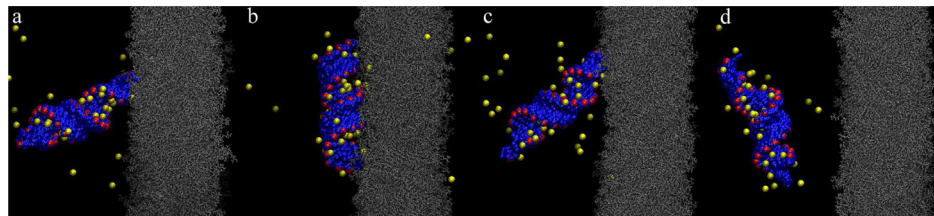


Figure 2. Snapshots of the siRNA–POPC-1 system: (a) 200, (b) 525, (c) 700, and (d) 775 ns. siRNA is shown in blue and red, lipids in gray, and Na^+ ions in yellow.

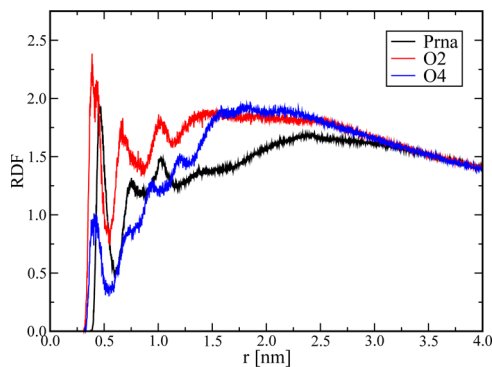


Figure 3. RDFs for nitrogen atoms Npc of choline moieties of POPC lipids and various atoms of a siRNA molecule. Shown are the results for siRNA phosphate atoms Prna and oxygen atoms O2 and O4 of uracil nucleotides. The averaging was performed over last 300 ns of the 800 ns trajectory.

of the unpaired nucleotides. Note that the terminal adenine–uracil base pairs of the siRNA duplex can undergo transient opening events (fraying),³⁶ so that we decided to include them to the group of overhanging terminal nucleotides and consider these two types of siRNA atoms together.

In Figure 4 (top), we show the time evolution of numbers of contacts of siRNA phosphate groups with lipid choline moieties. Because the total number of phosphate groups in the duplex exceeds considerably that in the terminal nucleotides, for the sake of clarity, we normalized the number

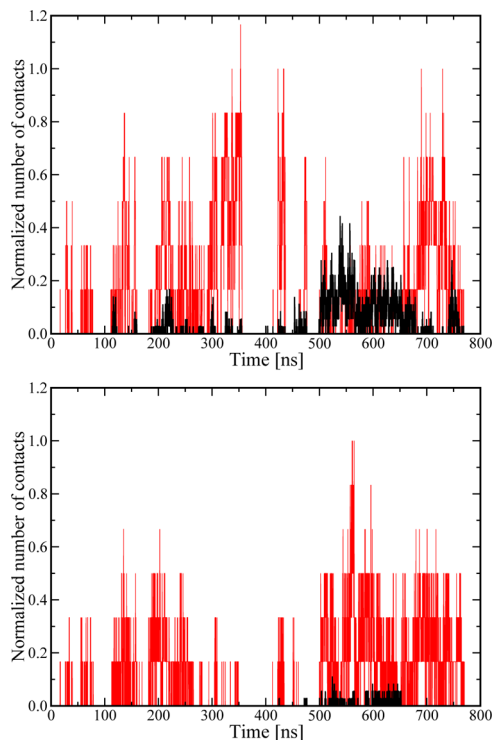


Figure 4. (Top) Normalized number of contacts of siRNA phosphate groups with lipid choline moieties as a function of time. Shown are the results for the siRNA duplex (black line) and for the terminal nucleotides (dsU)(ssUU) (red line). (Bottom) Normalized number of contacts of uracil oxygen atoms O2 (the duplex is shown in black, the terminal nucleotides in red) with lipid choline moieties as a function of time.

of contacts by the overall number of phosphates in each group. It is clearly seen that overhanging nucleotides of siRNA establish the contacts with lipid choline groups much more efficiently as compared to the nucleotides in the duplex. The average number of Prna–Npc contacts amounts approximately to 0.028 and 0.128 per phosphate group for the duplex and terminal nucleotides, respectively (the corresponding quantities for the siRNA–POPC-2 system were 0.018 and 0.058). Furthermore, we evaluated characteristic residence times of Prna–Npc contacts for both types of siRNA phosphates. Following to ref 24, the residence time for Prna–Npc contacts was estimated as the average time that a siRNA's phosphorus atom spends in the first coordination shell of a nitrogen atom of a choline lipid group. It turns out that the contacts of overhanging nucleotides with lipids are characterized by longer residence times as compared to the duplex: 0.64 ns versus 0.34 ns (0.62 ns vs 0.20 ns for the siRNA–POPC-2 system). All this supports our initial hypothesis that unpaired overhanging nucleotides play a crucial role in interactions of siRNA with lipids.

Another interesting observation consists of the fact that the overhanging nucleotides almost never bind to the bilayer surface simultaneously. Instead, the siRNA–bilayer interactions switch from one siRNA end to the other, the switching being observed for both phosphate and uracil oxygen atoms of the siRNA strand ends (see Figure S1). Binding of both “sticky ends” of siRNA is hypothetically possible when the siRNA duplex interacts with the bilayer surface, that is, within the time interval from 500 to 650 ns in Figure 4 (top). However, simultaneous binding of siRNA ends is not seen in this time domain either (Figure S1), most likely because the overhanging parts of siRNA strands are too short.

Relatively strong interactions of phosphate groups of overhanging unpaired nucleotides with lipid head groups [see Figures 3 and 4 (top)] allow us to assume that there might be other atomic groups of the nucleotides (in addition to phosphates), which could contribute to the siRNA–lipid binding. To this end, we carried out a thorough analysis of contacts between electronegative siRNA atoms and lipid choline moieties. From corresponding RDFs, we came to a conclusion that choline groups can establish contacts with siRNA sugar atoms as well as with electronegative atoms of the grooves. Because the overhanging unpaired nucleotides of the considered siRNA are uracils (and so is one of the nucleotides of terminal base pairs of the duplex), we focused mostly on this type of nucleotides. As an illustration, in Figure 3, we plot RDFs for uracil's oxygen atoms (O2 and O4) and choline moieties. The highest first peak is seen for O2 atoms, which is a sign that the O2–Npc interactions are stronger than the O4–Npc ones. The time evolution of the normalized number of the O2–Npc contacts clearly shows that terminal nucleotides are mainly involved in this type of interactions, whereas the contribution coming from the duplex is negligible [see Figure 4 (bottom)]. We note that similar behavior (but to a considerably lesser extent) was also observed for the contacts between choline groups and nitrogen atoms (N3 and N7) of the terminal adenines of the duplex (data not shown). To unlock the overall picture of choline–uracil interactions, in Figure 5, we plot the average numbers of contacts of lipid choline groups with various siRNA atoms of the terminal uracil nucleotides. Surprisingly, the contribution coming from siRNA sugar atoms somewhat exceeds the one from oxygen atoms of charged phosphate groups. In turn, the overall number of

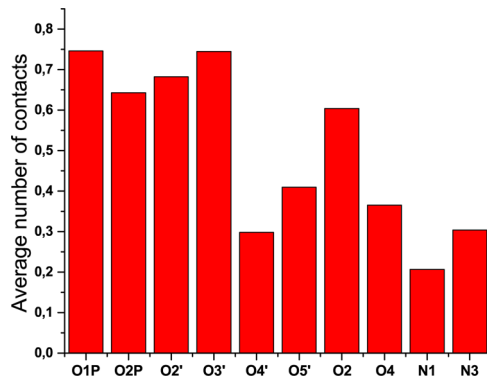


Figure 5. Average number of contacts of nitrogen atoms of lipid choline groups (Npc) with selected electronegative siRNA atoms of the terminal uracil nucleotides. The averaging was performed over the full 800 ns trajectory.

contacts of groove atoms with Npc is smaller than the above-mentioned atomic groups (phosphate and sugar atoms) but still noticeable (see Figure 5).

It is noteworthy that for the siRNA–POPC-2 system, we witnessed infrequent contacts of Npc atoms with Hoogsteen sites of guanine nucleotides (O6 and N7) that are present only in the duplex region of siRNA. It is likely that this type of siRNA–lipid contacts emerges when the siRNA duplex is in contact with the lipid/water interface and depends on the spatial orientation of the siRNA duplex within the bilayer (similar to the Ca-induced embedding of DNA into the lipid bilayer).²⁴

Interestingly, for one of the systems (siRNA–POPC-2), we witnessed noncanonical form of the terminal base pair (AU) of the duplex region. Such a noncanonical form (or the “fraying effect”), being poorly understood for RNA,³⁶ seems to be a result of siRNA binding to the lipid bilayer: the fraying emerges when the neighboring overhanging nucleotide U22-1 is anchored to the bilayer surface (at $t = 250$ ns). The noncanonical form lasted for ~ 280 ns and eventually returned to the canonical form.

Besides the interactions with lipid polar head groups, a siRNA molecule is surrounded by its counterions (Na^+ ions in our case). In general, it is known that Na^+ ions are localized around the RNA duplex (the A-form) to a larger degree as compared to the DNA duplex (the B-form) of the same sequence.³⁷ Stronger interactions with ions imply more efficient neutralization of the siRNA charge and correspondingly could affect the siRNA adsorption on the neutral lipid bilayer. We calculated the number of contacts of siRNA’s phosphate groups with Na^+ ions and found that only ~ 3 cations interact with siRNA (see Figures S2 and S3). In addition to Prna, sodium ions are found to interact also with electronegative atoms of the major groove such as Hoogsteen sites of adenine (N7) and guanine (N7 and O6) as well as oxygen atoms O4 of uracil (see Figure S3). Taken together with siRNA phosphate atoms, this gives us ~ 8 Na^+ ions bound on average to the siRNA molecule, so that we do not observe significant neutralization of the siRNA charge ($-42e$) by sodium ions.

To summarize this section, we can conclude that adsorption of a siRNA molecule on the surface of a zwitterionic phospholipid bilayer is mainly driven by the interactions between overhanging terminal nucleotides with polar lipid head groups (choline moieties). The region of the siRNA duplex can also contribute to some extend to lipid–siRNA interactions;

such siRNA duplex adsorption weakens interactions of the overhanging nucleotides with the bilayer.

Ca-Mediated Formation of siRNA–Phospholipid Complexes. The existence of “sticky ends” (overhanging unpaired nucleotides) seems to be an origin of the difference in binding of siRNA and DNA to the surface of neutral lipid bilayers: siRNA does adsorb on the bilayers (although its adsorption is rather weak and unstable), whereas DNA does not. In the case of DNA, both experimental^{14,39–41} and computational^{24,25} studies clearly demonstrated that the formation of stable DNA–zwitterionic lipid complexes can efficiently be promoted by adding divalent calcium ions into the aqueous solution. As the main part of a siRNA molecule also represents a polyanionic duplex, it is reasonable to anticipate similar Ca-induced effects for siRNA–lipid systems. To the best of our knowledge, there is still lack of experimental studies in this field, so that here we employ atomic-scale MD simulations to explore the impact of calcium ions on the interactions between siRNA and the POPC lipid bilayer. To this end, we carried out simulations of two siRNA–POPC systems in the presence of 100 mM of CaCl_2 salt (see Table 1). As the results turned out to be similar for both simulated systems, we chose to present findings for the siRNA–POPC–Ca-1 system only.

Visual inspection of the MD trajectories allows us to conclude that adding Ca^{2+} ions to the siRNA–POPC system does promote adsorption of a siRNA on the lipid bilayer, leading to the formation of a stable siRNA–lipid complex. To get insight into the mechanism of the complex formation, we explored various types of contacts between choline moieties of POPC lipids, Ca^{2+} ions, and phosphate groups of siRNA and lipids molecules [see Figure 6 (top)].

First of all, it is seen that the contacts between phosphate groups of siRNA and lipid choline moieties (Prna–Npc) appear already in the beginning of simulations, implying that the initial adsorption of siRNA on the bilayer is relatively fast. Nevertheless, the overall process of the adsorption converges very slowly: the number of Prna–Npc contacts reaches the equilibrium value of ~ 25 within 1 μs [see Figure 6 (top)]. It is noteworthy that this characteristic demonstrated considerably faster equilibration in the case of DNA under similar conditions (~ 400 ns).²⁴ As we proceed to show, this difference is mainly due to a rather complex binding pattern of Ca^{2+} ions to a siRNA molecule. Another important aspect is related to the role of the “sticky ends” and the duplex in the siRNA adsorption. It is obvious that the striking difference that was seen for the terminal and the duplex nucleotides in the Ca-free systems now vanishes [cf. Figures 4 (top) and 6 (top)]. The normalized number of Prna–Npc contacts for nucleotides of the siRNA duplex is much larger and more stable as compared to the Ca-free situation because Ca^{2+} ions dominate in the process of siRNA adsorption over the “sticky ends”. The average number of Prna–Npc contacts amounts to 0.53 ± 0.10 (0.55 ± 0.09 for the siRNA–POPC-2 system) choline groups per phosphate in the duplex [see Figure 6 (top)], which is a relatively high value, given that not all duplex nucleotides are able to bind to the lipid bilayer because of obvious geometrical limitations of the double-stranded helical motif.

The crucial role of divalent Ca^{2+} ions in siRNA adsorption on the zwitterionic lipid bilayer is clearly seen from the analysis of the number of contacts of Ca^{2+} ions with phosphate groups of POPC lipids and siRNA [see Figure 6 (top)]. Both these types of contacts develop very quickly after simulations start, within few nanoseconds. An increase in the number of Ca–Ppc

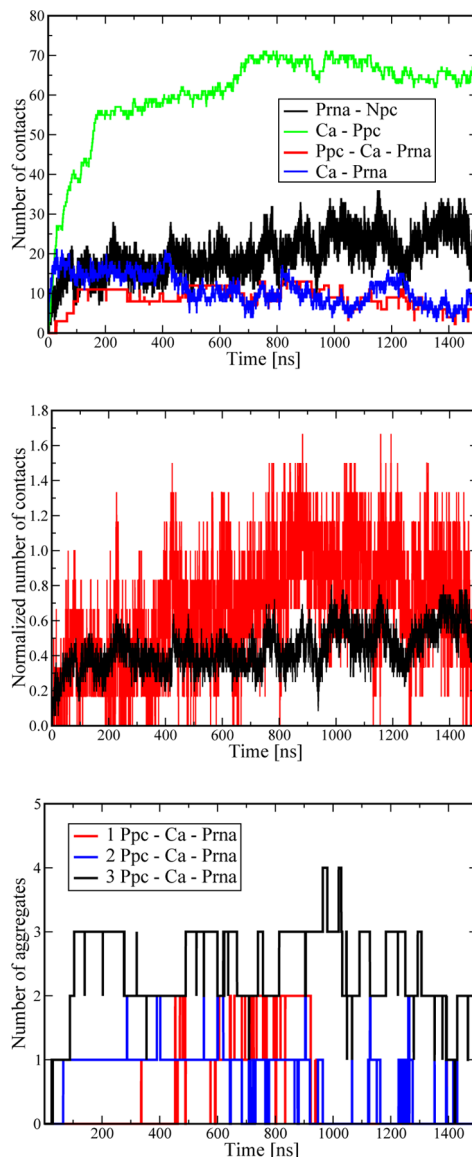


Figure 6. (Top) Number of contacts of siRNA phosphates with lipid choline groups (black line), the number of contacts of Ca^{2+} ions with phosphate groups of lipids (green line) and siRNA (blue line), and the number of Ca-mediated bridges between phosphates of lipids and siRNA phosphates (red line) as a function of time. (Middle) Normalized number of contacts of siRNA phosphate groups (the duplex, black line and the terminal nucleotides, red line) with lipid choline groups as a function of time. (Bottom) Number of Ca-mediated aggregates formed by siRNA and one (red line), two (blue line), and three (black line) lipid molecules as a function of time.

contacts indicates to adsorption of Ca^{2+} ions to the surface of a lipid bilayer. It takes around 700 ns for this process to fully equilibrate; the adsorbed cations make the zwitterionic lipid bilayer cationic, promoting the electrostatic attraction between the oppositely charged siRNA and the bilayer.

In turn, binding of Ca^{2+} ions to the siRNA molecule [Ca–Prna contacts in Figure 6 (top)] shows nontrivial behavior. In the beginning of simulations, $\sim 16 \text{ Ca}^{2+}$ ions (on average) get bound to siRNA phosphate groups and such a situation lasts for a rather long time. However, after ~ 400 ns, the number of Ca^{2+} ions bound to Prna drops to about 10. The most likely origin of such behavior is related to the way divalent calcium ions interact with the siRNA grooves.

It is well established that the main mode of binding of divalent ions to nucleic acids is related to the interaction of an ion with a phosphate group of the nucleic acid backbone. Wang et al. showed that magnesium ions are able to bind to phosphate groups of both strands of the duplex, making a bridge across the so-called “outer mouth” of the major groove.⁴² Importantly, such a situation is possible only for the duplex in the A-form (RNA) and not in the B-form (DNA) because the phosphates of the two strands are located closer to each other in the major groove of the A-form duplex.⁴³ Other experimental studies reported a significant narrowing of the major groove of RNA in the presence of Ca^{2+} ions, which was accompanied by a shorting of the duplex.^{44,45} Ordered Ca^{2+} ions were also found in the uracil-rich bulge region of an HIV-1 transactivation response region RNA fragment.⁴⁶ Therefore, it is instructive to analyze the binding of Ca^{2+} ions to siRNA in detail, with a particular focus on the ability of the cations to bridge phosphate groups of siRNA strands.

In Figure 7 (top), we plot the time evolution of the width of the major groove calculated for the siRNA nucleotide A12 with

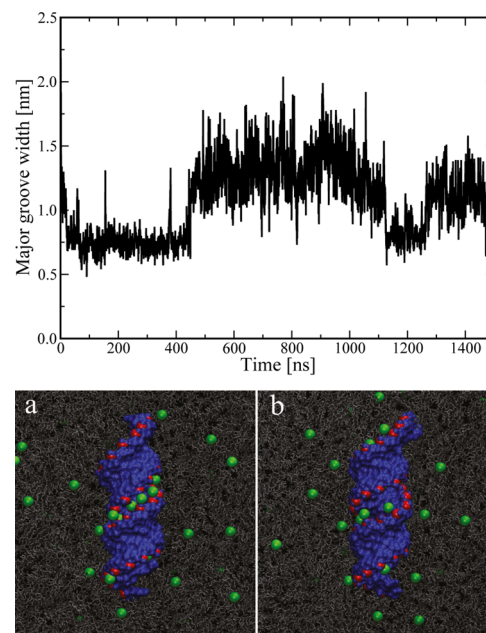


Figure 7. (Top) Width of the major groove calculated for the siRNA nucleotide A12 as a function of time. (Bottom) Snapshots of the siRNA–POPC– Ca^{2+} system at 300 (a) and 900 ns (b). siRNA is shown in blue and red, lipids in gray, and Ca^{2+} ions in green.

the use of the 3DNA suite.⁴⁷ Indeed, we witness a considerable narrowing of the major groove in the central part of siRNA. This narrowing, being accompanied by suppressed width fluctuations, remains stable for ~ 400 ns. Visual inspection of calcium ions bound to siRNA show that they indeed bridge both siRNA strands, leading to the narrowing of the major groove (see snapshot (a) in Figure 7 (bottom)). Thereby, we confirm that Ca^{2+} ions are able to form a “metal ion zipper” in the major groove of siRNA (similar to the one observed previously for Mg ions in ref 48). This ion zipper is destroyed at $t > 400$ ns because of progressive formation of the siRNA–lipid complex: Ca-mediated adsorption of siRNA on the lipid bilayer suppresses the interactions of siRNA with divalent ions and promotes ion unzipping. As a result, Ca^{2+} ions leave the major groove and the groove itself widens noticeably (see Figure 7).

This release of Ca^{2+} ions from the major groove explains the observed drop in the number of Ca–Prna contacts (see Figure 6 (top)). Remarkably, the unzipping of the major groove of siRNA seems to be reversible: one can observe a new narrowing of the groove with the time interval from 1100 to 1250 ns (see Figure 7 (top)). This narrowing is accompanied by some decrease in the number of contacts of Ca^{2+} ions with the POPC lipids [Figure 6 (top)].

Last but not least, Ca^{2+} ions turn out to be responsible not only for the initial electrostatic attraction between an anionic siRNA molecule and a lipid bilayer with the Ca-induced positive charge but also for the stabilization of the resulting siRNA–lipid complex. The mechanism of this stabilization is similar to what was observed for DNA:^{24,25} Ca^{2+} ions form “bridges” between phosphate groups of siRNA and lipid molecules. The number of such bridges was estimated by counting Ca^{2+} ions whose first hydration shells contain both siRNA and lipid phosphate atoms [see Figure 6 (top)]. What is more, the bridges do not link pairs of phosphate groups but rather create aggregates of different sizes. As seen in Figure 6 (bottom), after ~ 100 ns of initial equilibration, the aggregates consisting of a single phosphate group of siRNA and phosphates of three POPC lipids dominate in line with what was observed in DNA–lipid systems.^{24,25} However, there is a new feature that was not seen for DNA. After ~ 400 ns, one can observe the appearance of small Ca-mediated aggregates (siRNA–one lipid), which is a result of the above-mentioned unzipping of the major groove: additional Ca^{2+} ions from the outer mouth of the major groove enter the lipid/water interface and form these one-lipid aggregates. With time, these aggregates attach other lipid molecules and correspondingly increase in size, so that after $\sim 1 \mu\text{s}$, three-lipid aggregates again dominate [see Figure 6 (bottom)]. Thus, the “ion zipping” pattern of binding of Ca^{2+} ions to siRNA can affect the Ca-mediated siRNA–lipid interactions.

CONCLUSIONS

Liposome carriers for delivering siRNA into the cells are of tremendous importance because of an exceptionally high potential of the therapy based on the ability of siRNA to silence target genes. In addition to cationic lipids that were traditionally used for delivering nucleic acids, the efficiency of neutral (nontoxic) lipid molecules for siRNA delivery was recently demonstrated.^{12,13} Nevertheless, very little is known about the molecular mechanisms behind the interactions of siRNA with zwitterionic (neutral) lipids. The main goal of our paper is to contribute to this important field. To this end, we performed atomic-scale MD simulations of siRNA molecules interacting with phospholipid bilayers.

Our findings clearly demonstrate that siRNA does adsorb on the surface of a zwitterionic lipid bilayer, although its binding is rather weak and unstable. The siRNA adsorption is driven by the attractive interactions of overhanging terminal nucleotides with choline moieties of lipid molecules. The open conformations of the unpaired nucleotides allow lipid choline groups to access the oppositely charged phosphate groups of siRNA. Other electronegative atomic groups of these nucleotides (sugar and groove atoms) also contribute to the siRNA–lipid interactions to a noticeable extent. A typical binding mode of a nucleic acid is anchoring of one of the siRNA ends to the bilayer surface. A complete temporary detachment of a siRNA molecule and adsorption of the duplex part of siRNA are also observed; the latter is accompanied by

weakening of the interactions between siRNA ends and the bilayer surface. We emphasize that the existence of the overhanging nucleotides (“sticky ends”) is crucial for siRNA adsorption; their absence in the case of DNA is the underlying reason for a drastic difference in the ability of siRNA and DNA to adsorb on the bilayer surface: as it was shown earlier, the zwitterionic phospholipid bilayer represents a repulsive barrier for DNA molecules.²⁵ Overall, the observed binding of siRNA to the surface of a zwitterionic lipid bilayer is in good qualitative agreement with experimental data.^{12,13}

We also demonstrate that adding Ca^{2+} ions to the siRNA–POPC system promotes siRNA adsorption on the lipid bilayer, making siRNA–lipid interactions much more stronger. Such effects were reported earlier for DNA^{24,39} but not for RNA. Similar to DNA, we show that divalent cations adsorb on the zwitterionic lipid bilayer, inducing attractive interactions between the polyanionic siRNA molecule and the bilayer. Ca^{2+} ions are also responsible for stabilizing the resulting siRNA–lipid complex through the formation of Ca-mediated aggregates of siRNA and lipid molecules. Therefore, unlike in the calcium-free situation, divalent cations dominate in adsorption over terminal unpaired nucleotides. In contrast to DNA, siRNA is characterized by the A-form and correspondingly by a narrower major groove. Interactions of Ca^{2+} ions with siRNA are found to lead to the appearance of the so-called “ion zipper” when ions reside on the outer mouth of the groove. Importantly, unzipping of the major groove results in the release of divalent ions from the groove of siRNA to the lipid/water interface and therefore affects directly the Ca-mediated lipid–siRNA interactions.

Overall, our computational findings contribute significantly to a deeper understanding of the structure and function of liposome carriers used for siRNA delivery into target cells. They can be used as a basis for rational design of novel biocompatible delivery systems to improve the current state of siRNA-based therapeutics. In particular, future experimental studies could explore the enhanced binding of siRNA to the phospholipid bilayer surface because of the presence of divalent cations, which was first observed in our work. Calcium ions could result in the formation of ordered lipid–siRNA structures and multilamellar siRNA-mediated vesicles; such structural changes can easily be detected with the use of the state-of-the-art experimental techniques.^{15,49}

ASSOCIATED CONTENT

S Supporting Information

The Supporting Information is available free of charge on the ACS Publications website at DOI: [10.1021/acs.langmuir.8b01211](https://doi.org/10.1021/acs.langmuir.8b01211).

Contributions of siRNA strand ends to the normalized number of contacts of siRNA atoms with lipid choline moieties; the number of contacts of Na^+ ions with various siRNA’s atoms; and RDFs for Na^+ ions and electronegative atoms of siRNA ([PDF](#))

AUTHOR INFORMATION

Corresponding Author

*E-mail: a.gurtovenko@gmail.com. Web: biosimu.org. Phone: +7-812-3285601. Fax: +7-812-3286869.

ORCID

Andrey A. Gurtovenko: [0000-0002-9834-1617](#)

Notes

The authors declare no competing financial interest.

ACKNOWLEDGMENTS

The authors wish to acknowledge the use of the computer cluster of the Institute of Macromolecular Compounds RAS and the Lomonosov supercomputer at the Moscow State University. This work was supported by the Presidium of the Russian Academy of Sciences through the grant program “Molecular and Cellular Biology” and by the Russian Foundation of Basic Research through grant 17-03-00446.

REFERENCES

- (1) Fire, A.; Xu, S.; Montgomery, M. K.; Kostas, S. A.; Driver, S. E.; Mello, C. C. Potent and specific genetic interference by double-stranded RNA in *Caenorhabditis elegans*. *Nature* **1998**, *391*, 806.
- (2) Sullenger, B. A.; Nair, S. From the RNA world to the clinic. *Science* **2016**, *352*, 1417–1420.
- (3) Bobbin, M. L.; Rossi, J. J. RNA interference (RNAi)-based therapeutics: delivering on the promise? *Annu. Rev. Pharmacol. Toxicol.* **2016**, *56*, 103–122.
- (4) Mintzer, M. A.; Simanek, E. E. Nonviral vectors for gene delivery. *Chem. Rev.* **2009**, *109*, 259–302.
- (5) Guo, X.; Huang, L. Recent advances in nonviral vectors for gene delivery. *Acc. Chem. Res.* **2011**, *45*, 971–979.
- (6) Yin, H.; Kanasty, R. L.; Eltoukhy, A. A.; Vegas, A. J.; Dorkin, J. R.; Anderson, D. G. Non-viral vectors for gene-based therapy. *Nat. Rev. Genet.* **2014**, *15*, 541.
- (7) Whitehead, K. A.; Dorkin, J. R.; Vegas, A. J.; Chang, P. H.; Veiseh, O.; Matthews, J.; Fenton, O. S.; Zhang, Y.; Olejnik, K. T.; Yesilyurt, V.; Chen, D.; Barros, S.; Klebanov, B.; Novobrantseva, T.; Langer, R.; Anderson, D. G. Degradable lipid nanoparticles with predictable in vivo siRNA delivery activity. *Nat. Commun.* **2014**, *5*, 4277.
- (8) Juliano, R. L. The delivery of therapeutic oligonucleotides. *Nucleic Acids Res.* **2016**, *44*, 6518–6548.
- (9) Xia, Y.; Tian, J.; Chen, X. Effect of surface properties on liposomal siRNA delivery. *Biomaterials* **2016**, *79*, 56–68.
- (10) Xue, H. Y.; Liu, S.; Wong, H. L. Nanotoxicity: a key obstacle to clinical translation of siRNA-based nanomedicine. *Nanomedicine* **2014**, *9*, 295–312.
- (11) Li, W.; Szoka, F. C. Lipid-based nanoparticles for nucleic acid delivery. *Pharm. Res.* **2007**, *24*, 438–449.
- (12) Ozpolat, B.; Sood, A. K.; Lopez-Berestein, G. Liposomal siRNA nanocarriers for cancer therapy. *Adv. Drug Delivery Rev.* **2014**, *66*, 110–116.
- (13) Landen, C. N.; Chavez-Reyes, A.; Bucana, C.; Schmandt, R.; Deavers, M. T.; Lopez-Berestein, G.; Sood, A. K. Therapeutic EphA2 gene targeting in vivo using neutral liposomal small interfering RNA delivery. *Cancer Res.* **2005**, *65*, 6910–6918.
- (14) Gromelski, S.; Brezesinski, G. DNA condensation and interaction with zwitterionic phospholipids mediated by divalent cations. *Langmuir* **2006**, *22*, 6293–6301.
- (15) Ainalem, M.-L.; Kristen, N.; Edler, K. J.; Höök, F.; Sparr, E.; Nylander, T. DNA binding to zwitterionic model membranes. *Langmuir* **2010**, *26*, 4965–4976.
- (16) Dabkowska, A. P.; Barlow, D. J.; Clifton, L. A.; Hughes, A. V.; Webster, J. R. P.; Green, R. J.; Quinn, P. J.; Lawrence, M. J. Calcium-mediated binding of DNA to 1, 2-distearoyl-sn-glycero-3-phosphocholine-containing mixed lipid monolayers. *Soft Matter* **2014**, *10*, 1685–1695.
- (17) Pisani, M.; Mobbili, G.; Placentino, I. F.; Smorlesi, A.; Bruni, P. Biophysical Characterization of Complexes of DNA with Mixtures of the Neutral Lipids 1, 2-Dioleoyl-sn-glycero-3-phosphoethanolamine-N-hexanoylamine or 1, 2-Dioleoyl-sn-glycero-3-phosphoethanolamine-N-dodecanoyleamine and 1, 2-Dioleoyl-sn-glycero-3-phosphocholine in the Presence of Bivalent Metal Cations for DNA Transfection. *J. Phys. Chem. B* **2011**, *115*, 10198–10206.
- (18) Das, A.; Adhikari, C.; Chakraborty, A. Interaction of different divalent metal ions with lipid bilayer: impact on the encapsulation of doxorubicin by lipid bilayer and lipoplex mediated deintercalation. *J. Phys. Chem. B* **2017**, *121*, 1854–1865.
- (19) Karatasos, K.; Posocco, P.; Laurini, E.; Prich, S. Poly (amidoamine)-based Dendrimer/siRNA Complexation Studied by Computer Simulations: Effects of pH and Generation on Dendrimer Structure and siRNA Binding. *Macromol. Biosci.* **2012**, *12*, 225–240.
- (20) Sun, C.; Tang, T.; Uludag, H. A molecular dynamics simulation study on the effect of lipid substitution on polyethylenimine mediated siRNA complexation. *Biomaterials* **2013**, *34*, 2822–2833.
- (21) Pavan, G. M.; Mintzer, M. A.; Simanek, E. E.; Merkel, O. M.; Kissel, T.; Danani, A. Computational insights into the interactions between DNA and siRNA with “rigid” and “flexible” triazine dendrimers. *Biomacromolecules* **2010**, *11*, 721–730.
- (22) Breton, M.; Delemotte, L.; Silve, A.; Mir, L. M.; Tarek, M. Transport of siRNA through lipid membranes driven by nanosecond electric pulses: an experimental and computational study. *J. Am. Chem. Soc.* **2012**, *134*, 13938–13941.
- (23) Choubey, A.; Nomura, K.-i.; Kalia, R. K.; Nakano, A.; Vashishta, P. Small interfering ribonucleic acid induces liquid-to-ripple phase transformation in a phospholipid membrane. *Appl. Phys. Lett.* **2014**, *105*, 113702.
- (24) Antipina, A. Y.; Gurtovenko, A. A. Molecular mechanism of calcium-induced adsorption of DNA on zwitterionic phospholipid membranes. *J. Phys. Chem. B* **2015**, *119*, 6638–6645.
- (25) Antipina, A. Y.; Gurtovenko, A. A. Molecular-level insight into the interactions of DNA with phospholipid bilayers: barriers and triggers. *RSC Adv.* **2016**, *6*, 36425–36432.
- (26) Cornell, W. D.; Cieplak, P.; Bayly, C. I.; Gould, I. R.; Merz, K. M.; Ferguson, D. M.; Spellmeyer, D. C.; Fox, T.; Caldwell, J. W.; Kollman, P. A. A second generation force field for the simulation of proteins, nucleic acids, and organic molecules. *J. Am. Chem. Soc.* **1995**, *117*, 5179–5197.
- (27) Zgarbová, M.; Otyepka, M.; Šponer, J. ī.; Mládek, A.; Banáš, P.; Cheatham, T. E., III; Jurecka, P. Refinement of the Cornell et al. nucleic acids force field based on reference quantum chemical calculations of glycosidic torsion profiles. *J. Chem. Theory Comput.* **2011**, *7*, 2886–2902.
- (28) Pérez, A.; Marchán, I.; Svozil, D.; Sponer, J.; Cheatham, T. E.; Laughton, C. A.; Orozco, M. Refinement of the AMBER force field for nucleic acids: improving the description of α/γ conformers. *Biophys. J.* **2007**, *92*, 3817–3829.
- (29) Dickson, C. J.; Madej, B. D.; Skjevik, Å. A.; Betz, R. M.; Teigen, K.; Gould, I. R.; Walker, R. C. Lipid14: the amber lipid force field. *J. Chem. Theory Comput.* **2014**, *10*, 865–879.
- (30) Jorgensen, W. L.; Chandrasekhar, J.; Madura, J. D.; Impey, R. W.; Klein, M. L. Comparison of simple potential functions for simulating liquid water. *J. Chem. Phys.* **1983**, *79*, 926–935.
- (31) Bussi, G.; Donadio, D.; Parrinello, M. Canonical sampling through velocity rescaling. *J. Chem. Phys.* **2007**, *126*, 014101.
- (32) Berendsen, H. J. C.; Postma, J. P. M.; van Gunsteren, W. F.; DiNola, A.; Haak, J. R. Molecular dynamics with coupling to an external bath. *J. Chem. Phys.* **1984**, *81*, 3684–3690.
- (33) Essmann, U.; Perera, L.; Berkowitz, M. L.; Darden, T.; Lee, H.; Pedersen, L. G. A smooth particle mesh Ewald method. *J. Chem. Phys.* **1995**, *103*, 8577–8593.
- (34) Hess, B.; Kutzner, C.; van der Spoel, D.; Lindahl, E. GROMACS 4: algorithms for highly efficient, load-balanced, and scalable molecular simulation. *J. Chem. Theory Comput.* **2008**, *4*, 435–447.
- (35) Kučerka, N.; Nieh, M.-P.; Katsaras, J. Fluid phase lipid areas and bilayer thicknesses of commonly used phosphatidylcholines as a function of temperature. *Biochim. Biophys. Acta* **2011**, *1808*, 2761–2771.
- (36) Zgarbová, M.; Otyepka, M.; Šponer, J.; Lankaš, F.; Jurečka, P. Base pair fraying in molecular dynamics simulations of DNA and RNA. *J. Chem. Theory Comput.* **2014**, *10*, 3177–3189.

- (37) Pan, F.; Roland, C.; Sagui, C. Ion distributions around left-and right-handed DNA and RNA duplexes: a comparative study. *Nucleic Acids Res.* **2014**, *42*, 13981–13996.
- (38) Gurtovenko, A. A.; Vattulainen, I. Effect of NaCl and KCl on phosphatidylcholine and phosphatidylethanolamine lipid membranes: Insight from atomic-scale simulations for understanding salt-induced effects in the plasma membrane. *J. Phys. Chem. B* **2008**, *112*, 1953–1962.
- (39) McManus, J. J.; Rädler, J. O.; Dawson, K. A. Does calcium turn a zwitterionic lipid cationic? *J. Phys. Chem. B* **2003**, *107*, 9869–9875.
- (40) McManus, J. J.; Rädler, J. O.; Dawson, K. A. Phase behavior of DPPC in a DNA-calcium-zwitterionic lipid complex studied by small-angle X-ray scattering. *Langmuir* **2003**, *19*, 9630–9637.
- (41) Mengistu, D. H.; Bohinc, K.; May, S. Binding of DNA to zwitterionic lipid layers mediated by divalent cations. *J. Phys. Chem. B* **2009**, *113*, 12277–12282.
- (42) Robinson, H.; Gao, Y.-G.; Sanishvili, R.; Joachimiak, A.; Wang, A. H.-J. Hexahydrated magnesium ions bind in the deep major groove and at the outer mouth of A-form nucleic acid duplexes. *Nucleic Acids Res.* **2000**, *28*, 1760–1766.
- (43) Hud, N. V. *Nucleic Acid–Metal Ion Interactions*; Royal Society of Chemistry, 2009.
- (44) Ennifar, E.; Walter, P.; Dumas, P. A crystallographic study of the binding of 13 metal ions to two related RNA duplexes. *Nucleic Acids Res.* **2003**, *31*, 2671–2682.
- (45) Schaffer, M.; Peng, G.; Spingler, B.; Schnabl, J.; Wang, M.; Olieric, V.; Sigel, R. The X-ray structures of six octameric RNA duplexes in the presence of different di- and trivalent cations. *Int. J. Mol. Sci.* **2016**, *17*, 988.
- (46) Ippolito, J. A.; Steitz, T. A. A 1.3-Å resolution crystal structure of the HIV-1 trans-activation response region RNA stem reveals a metal ion-dependent bulge conformation. *Proc. Natl. Acad. Sci. U.S.A.* **1998**, *95*, 9819–9824.
- (47) Lu, X.-J.; Olson, W. K. 3DNA: a software package for the analysis, rebuilding and visualization of three-dimensional nucleic acid structures. *Nucleic Acids Res.* **2003**, *31*, 5108–5121.
- (48) Correll, C. C.; Freeborn, B.; Moore, P. B.; Steitz, T. A. Metals, motifs, and recognition in the crystal structure of a 5S rRNA domain. *Cell* **1997**, *91*, 705–712.
- (49) McManus, J. J.; Rädler, J. O.; Dawson, K. A. Observation of a rectangular columnar phase in a DNA-calcium-zwitterionic lipid complex. *J. Am. Chem. Soc.* **2004**, *126*, 15966–15967.